Cross-well seismic modeling with inclusion of tube waves and tube-wave-related arrivals

Chunling Wu and Jerry M. Harris

Department of Geophysics, Stanford University, Stanford, California, USA

Received 2 March 2004; revised 6 May 2004; accepted 11 May 2004; published 9 June 2004.

[1] Cross-well seismic data often contain strong tube waves and tube-wave-related arrivals due to the effects of the presence of two boreholes. A basic requirement for accurate cross-well seismic modeling and data processing is inclusion of these events. We use a 2-D velocity-stress variable-grid finite-difference parallel code for efficient cross-well field data modeling with inclusion of the two perforated cased boreholes. The synthetics resemble the field observations in terms of arrival times not only on P- and S-waves but also on tube waves and tube-wave-related secondary arrivals generated by perforations in the receiver and source wells. This study demonstrates that including boreholes into the modeling scheme can distinguish tube-wave-related events on seismograms to better assist data analysis and to guide data processing and interpretation. *INDEX TERMS:* 0902 Exploration Geophysics: Computational methods, seismic; 0915 Exploration Geophysics: Downhole methods; 0935 Exploration Geophysics: Seismic methods (3025); 3210 Mathematical Geophysics: Modeling; 3230 Mathematical Geophysics: Numerical solutions. **Citation:** Wu, C., and J. M. Harris (2004), Cross-well seismic modeling with inclusion of tube waves and tube-wave-related arrivals, *Geophys. Res. Lett.*, *31*, L11606, doi:10.1029/2004GL019873.

1. Introduction

[2] Cross-well seismic technology involves placing a seismic source in one well and a hydrophone string in another well. This technique has been widely used for reservoir and waste site characterization because it can provide high resolution images about subsurface. However, the presence of two boreholes has significant effects on the field data. Many of the strongest signals observed are modes traveling within the borehole: these tube waves are often sufficient to cloak the lower amplitude reflections and transmissions. Moreover, tube waves can re-radiate energy into the formation at changes along the borehole to generate tube-wave-related secondary arrivals [*Balch and Lee*, 1984]. To better understand wave patterns observed in the field data and to guide data processing and interpretation, accurate cross-well seismic modeling with inclusion of these events is desirable.

[3] Explicit finite-difference (FD) methods have historically dominated elastic wavefield modeling in geophysics because of their flexibility in representing complex models and their computational efficiency. However, to resolve small-scale boreholes (20–30 cm in diameter) within a large model (200–300 m in distance separating two boreholes) by a commonly used regular grid FD method requires too much memory for simulation on most computers. Variable-grid FD techniques [*Moczo*, 1989; *Jastram and Behle*, 1991; *Pitarka*, 1999], which allow the use of fine grid spacing in the vicinity of boreholes and coarse grid spacing in the field away from the boreholes, overcome the problem and have been applied to borehole seismic modeling [*Falk et al.*, 1996; *Wu et al.*, 2001].

[4] We use a 2-D velocity-stress optimized variable-grid FD parallel code [*Wu and Harris*, 2004] to efficiently model the cross-well seismic field data from West Texas with inclusion of the two perforated cased boreholes. Comparison between the synthetic and observed data shows that a good agreement has been achieved not only on direct P- and S-arrivals, but also on tube waves and tube-wave-related events.

2. Methods

[5] Following *Virieux* [1986], the 2-D velocity-stress elastic wave equation suitable for a staggered-grid FD scheme can be written as

$$\begin{aligned}
\rho\frac{\partial v_x}{\partial t} &= \frac{\partial \tau_{xx}}{\partial x} + \frac{\partial \tau_{xz}}{\partial z} \\
\rho\frac{\partial v_z}{\partial t} &= \frac{\partial \tau_{xz}}{\partial x} + \frac{\partial \tau_{zz}}{\partial z} \\
\frac{\partial \tau_{xx}}{\partial t} &= (\lambda + 2\mu)\frac{\partial v_x}{\partial x} + \lambda\frac{\partial v_z}{\partial z} \\
\frac{\partial \tau_{zz}}{\partial t} &= (\lambda + 2\mu)\frac{\partial v_z}{\partial z} + \lambda\frac{\partial v_x}{\partial x} \\
\frac{\partial \tau_{xz}}{\partial t} &= \mu\left(\frac{\partial v_x}{\partial z} + \frac{\partial v_z}{\partial x}\right)
\end{aligned} \tag{1}$$

where v_x and v_z are the particle velocity components; τ_{xx}, τ_{xz}, and τ_{zz} are stress components; ρ is density; λ and μ are *Lamé* coefficients.

[6] We use a simple FD gridding scheme to represent the x-z borehole plane. The plane is partitioned into: (1) domains of fine grid spacing for resolving boreholes and casings, (2) domains of coarse grid spacing constrained by the shortest wavelength in the medium, and (3) transition regions where the grid spacing smoothly varies between these extremes (see Figure 1). The smooth refinement from the coarse grid to fine grid avoids spurious reflection problems associated with sudden changes in the grid.

[7] Solving the elastic wave equation on a variable grid requires the spatial derivatives in equation (1) to be approximated using a stretched stencil. Several techniques exist for efficiently calculating the coefficients for the stretched difference operators. We use the optimized variable-grid FD method [*Wu and Harris*, 2004] to pre-compute explicit fourth-order operators for all spatial locations. Since the

0094-8276/04/2004GL019873

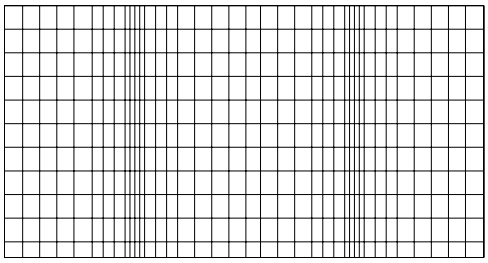

Figure 1. Variable-grid mesh for a cross-well model. The horizontal grid spacing is variable to accommodate small-scale boreholes with casing and cement in a large model.

mesh is only distorted along the x and z axis, coefficients are invariant along grid lines, reducing the memory required for stencil storage. The variable mesh is also staggered to increase stability and minimize numerical dispersion: a staggered scheme is crucial for handling the solid-liquid contact present at the borehole. Time derivatives are staggered across the velocity and stress variables and are approximated using an explicit second-order central difference operator.

[8] Spatial discretization (h) and temporal increments Δt are chosen to minimize dispersion and maintain stability during the computations. In particular, the inequalities

$$h_{\max} < \frac{V_{\min}}{5 f_{\max}} \tag{2}$$

$$\Delta t < \frac{0.606 h_{\min}}{V_{\max}}, \tag{3}$$

are enforced, where $h_{\min}$ and $h_{\max}$ are minimum and maximum grid spacing; $f_{\max}$ is the maximum frequency of the propagating signal, and $V_{\min}$ and $V_{\max}$ are the lowest and highest velocities in the media, respectively.

[9] To minimize artificial reflections at the boundaries of the computational domain, sponge absorbing boundary conditions [*Cerjan et al.*, 1985] are used at the edges of the model.

[10] A parallel version of the algorithm has been developed for more efficient calculations on a "Linux Beowulf" cluster. The parallel implementation utilizes spatial domain decomposition: different portions of the 2-D grid are allocated to different processors so that calculations within each subdomain take place synchronously. Sufficient overlap between adjacent subdomains/processors must be provided so that the fourth-order spatial FD operators can address all dependent variables at their particular staggered-grid storage locations. Inter-processor data communication is based on the MPI (Message Passing Interface).

3. Field Data Analysis and Modeling Study

[11] The cross-well field data we are analyzing and modeling were collected in the Permian Basin, West Texas. Two cased boreholes with 640 ft separation were used. The source well and receiver well have perforations at the depth of 9000 ft and 8930 ft, respectively.

3.1. Field Data Analysis

[12] Figure 2 shows a common-shot gather from this survey. The source is at depth 8695 ft with receiver sampling interval of 5 ft. The depth of the receivers ranges from 8190 to 9200 ft. In this data, in addition to direct P- and S-waves (P, S), strong tube waves (PT, ST, TPT, TST) and tube-wave-related secondary P and S arrivals (TP, TS) are observed. The tube waves and the secondary body

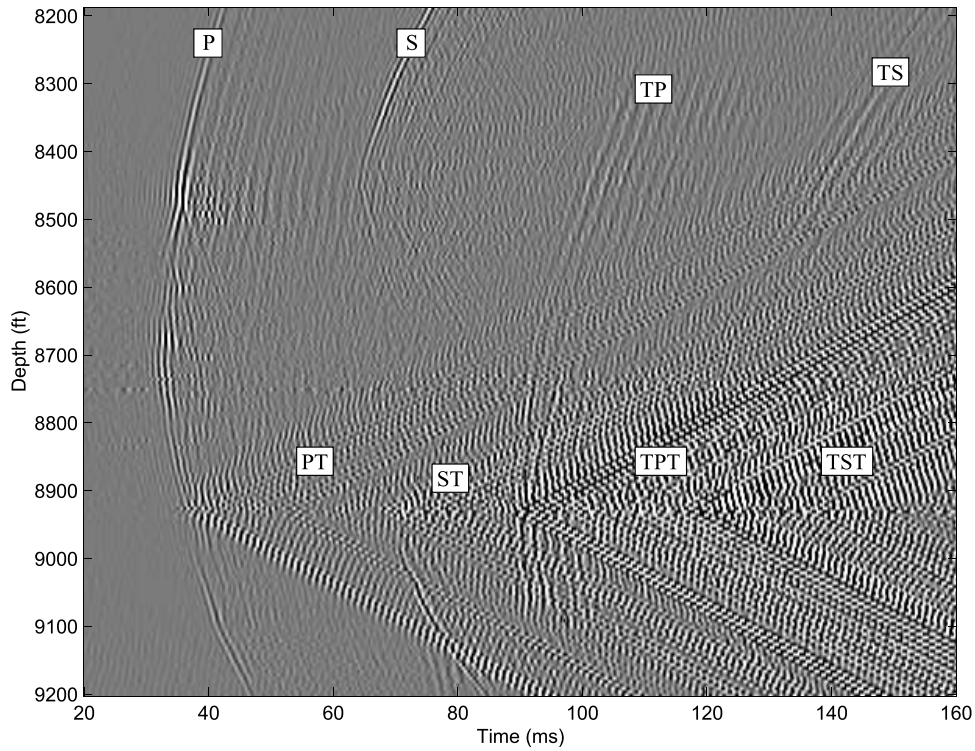

Figure 2. A common-shot gather of the cross-well survey from West Texas. The source depth is 8695 feet.

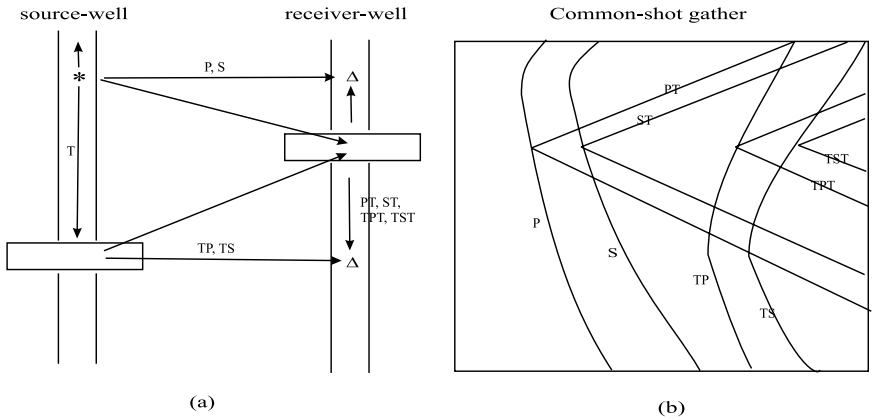

Figure 3. Schematic diagram of waves in the cross-well survey: (a) Ray paths; (b) Arrivals in the seismogram. P and S are the direct P- and S-waves. TP and TS are the secondary P and S-waves radiated by the source tube waves (T) at the perforations in the source well. PT, ST and TPT, TST are receiver tube waves generated by the direct and secondary body waves at the perforations in the receiver well.

waves observed in the common-shot gather are caused by the borehole perforations [*Mo and Harris*, 1995]. Perforations act as impedance discontinuities in a borehole. Impedance discontinuities in the source well cause tube waves to radiate body waves; impedance discontinuities in the receiver well cause tube waves to be generated by body wave interactions [*Balch and Lee*, 1984].

[13] Figure 3 schematically illustrates the ray paths (Figure 3a) and the associated arrivals in the seismogram (Figure 3b) of a common-shot gather. In the source well, the source excites body waves (P, S), and also excites tube waves (T) propagating along the source well. When the tube waves hit the perforations in the source well, they radiate energy into the formation to generated tube-wave-related body waves (TP, TS). When the body waves (P, S, TP, TS) impinge upon the receiver well, strong tube waves (PT, ST, TPT, TST) are excited at the perforations and propagate along the receiver well to be recorded.

[14] To test this data analysis requires including boreholes, casings and perforations into the modeling scheme.

3.2. Modeling Study

[15] The 2-D optimized variable-grid FD parallel code is used to model the common shot gather showed in Figure 2 with inclusion of the two perforated cased boreholes. The model is based on the survey geometry. P-wave velocities of the formation are obtained from the blocked P-wave velocity log in the source well (Figure 4a). The corresponding S-wave velocities are calculated by $V_s = V_p/\sqrt{3}$. The densities are obtained by $\rho = 0.23V_p^{0.25}$ [*Gardner et al.*, 1974]. Note in this latter equation, the unit of ρ is g/cm^3 and the unit of V_p is ft/s. Two perforated cased boreholes are

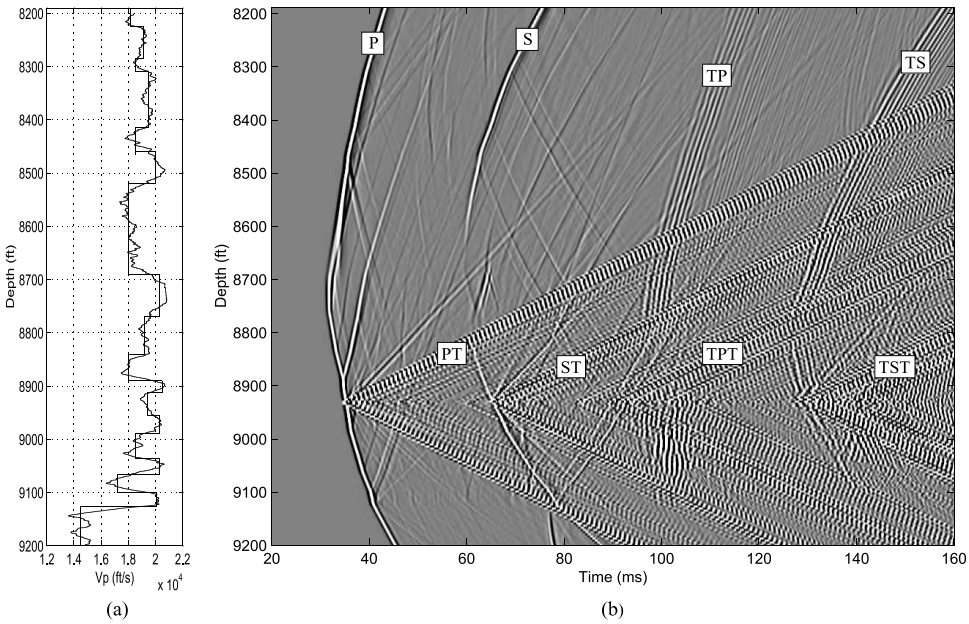

Figure 4. (a) Blocked V_p log from the source well; (b) Synthetic seismogram generated by 2-D variable-grid FD elastic modeling. See color version of this figure in the HTML.

embedded in the layered formation. The parameters for the two boreholes are the same: the diameter is 7.2 inch, water-filled, the thicknesses of the casing and cement are 0.6 inch and 1.2 inch, respectively. Perforations are represented by a small rectangular hole cut through the casing, cement and into the formation. Figure 1 schematically illustrates the computational mesh used for the model. In the vicinity of the well, the lateral grid spacing smoothly increases from 0.05 ft to 1 ft over a transition region of 1.8 ft wide. The vertical spacing is 1 ft throughout the grid. The total grid size for this variable-grid mesh is $NX \times NZ = 742 \times 1151$ which is less than 5% of the total grid size of a regular mesh with constant dx = 0.05 ft in the entire model ($NX \times NZ = 14980 \times 1151$); therefore, the computer memory requirements are greatly reduced by the variable-grid approach. Spectral analysis reveals that the frequencies in the field data are from 400 Hz to 1200 Hz. We use a Ricker wavelet with 800 Hz central frequency as the source function to excite the model. The calculations were performed on a 16 processor distributed "Linux Beowulf" cluster. One run of 110,000 time steps for the 742×1151 size model takes about 3 hours CPU time.

[16] The synthetic seismogram of the common shot gather is shown in Figure 4b. We see that all the identified arrivals in the field data (Figure 2): direct waves (P, S), tube-wave-related arrivals (TP, TS) and strong tube waves (PT, ST, TPT, TST) are observed in the synthetic seismogram. There is a good match between the synthetic and the field observations for these events, especially the kinematics. This modeling result supports the previous data analysis and can be used to guide the later phase of data processing such as tube wave attenuation.

[17] Though tube wave characteristics are similar in 2-D and 3-D [*Paillet and White*, 1982], our modeling results only qualitatively capture dynamic features because of the 2-D approximation on both tube waves and body waves. The difference between the synthetic and field observations in relative amplitude of some events (PT, ST, and interface reflections) is due not only to the 2-D approximation, but may be due in part to attenuation in the real earth. Extending to 3-D and introducing attenuation could achieve a better quantitative comparison.

4. Conclusions

[18] A 2-D velocity-stress optimized variable-grid FD parallel code has been used for efficiently modeling the cross-well seismic field data from West Texas with inclusion of two perforated cased boreholes. The synthetic data not only match the direct P- and S-arrivals in the field observations, but also fit the tube waves and tube-wave-related events generated by the perforations in the source and receiver wells. This study demonstrates that inclusion of boreholes into the modeling scheme can capture tube-wave-related phenomena on seismograms to better assist data analysis and to guide data processing and interpretation.

[19] Profitable directions for future research include extension of our modeling code to 3-D and the introduction of intrinsic attenuation. Both additions would allow a more quantitative prediction of amplitudes for borehole modes and body waves.

[20] **Acknowledgments.** We thank two anonymous reviewers for many helpful comments that significantly improved this manuscript. And, thanks to the industrial affiliates of the Stanford Seismic Tomography Project for providing the field data.

References

Balch, A. H., and M. W. Lee (1984), Vertical seismic profiling: Technique, applications, and case histories, report, Int. Human Resour. Develop. Corp., Boston, Mass.

Cerjan, C., D. Kosloff, R. Kosloff, and M. Reshef (1985), A nonreflecting boundary condition for discrete acoustic and elastic wave equations, *Geophysics*, *50*, 705–708.

Falk, P., E. Tessmer, and D. Gajewski (1996), Tube wave modeling by the finite-difference method with varying grid spacing, *Pure Appl. Geophys.*, *148*, 77–92.

Gardner, G. H. F., L. W. Gardner, and A. R. Gregory (1974), The diagnostic basis for stratigraphic straps, *Geophysics*, *39*, 770–780.

Jastram, C., and A. Behle (1991), Elastic modeling by finite-difference and the rapid expansion method (REM), paper presented at the 61st Annual International Meeting, Soc. of Explor. Geophys., Houston, Tex.

Mo, L., and J. M. Harris (1995), Analysis and attenuation of tube waves in crosswell seismic survey, paper presented at the 65th Annual International Meeting, Soc. of Explor. Geophys., Houston, Tex.

Moczo, P. (1989), Finite-difference technique for SH waves in 2-D media using irregular grids—Application to the seismic response problem, *Geophys. J. Int.*, *99*, 321–329.

Paillet, F. L., and J. E. White (1982), Acoustic modes propagation in the borehole and their relationship to rock properties, *Geophysics*, *47*, 1215–1228.

Pitarka, A. (1999), 3D elastic finite-difference modeling of seismic motion using staggered grids with nonuniform spacing, *Bull. Seismol. Soc. Am.*, *89*, 54–68.

Virieux, J. (1986), P-SV wave propagation in heterogeneous media: Velocity-stress finite-difference method, *Geophysics*, *51*, 889–901.

Wu, C., and J. M. Harris (2004), An optimized variable-grid finite-difference method for seismic forward modeling, *J. Seismic Explor.*, *12*, 343–353.

Wu, C., J. M. Harris, and J. Franklin (2001), Single-well seismic modeling in viscoelastic media using a variable-grid finite-difference method, paper presented at the 71st Annual International Meeting, Soc. of Explor. Geophys., San Antonio, Tex.

C. Wu and J. M. Harris, Department of Geophysics, Stanford University, 397 Panama Mall, Stanford, CA 94305, USA. (clwu@pangea.stanford.edu)